Palaeogeography, Palaeoclimatology, Palaeoecology 297 (2010) 621–632

Contents lists available at ScienceDirect

Palaeogeography, Palaeoclimatology, Palaeoecology

journal homepage: www.elsevier.com/locate/palaeo

Paleoenvironmental implications of an extensive maceriate microbialite bed in the Furongian Chaomidian Formation, Shandong Province, China

Jeong-Hyun Lee [a], Jitao Chen [a,b], S.K. Chough [a,*]

[a] School of Earth and Environmental Sciences, Seoul National University, Seoul 151-747, Republic of Korea
[b] College of Geological Science and Engineering, Shandong University of Science and Technology, Qingdao 266510, China

ARTICLE INFO

Article history:
Received 2 March 2010
Received in revised form 11 September 2010
Accepted 14 September 2010
Available online 18 September 2010

Keywords:
Microbialite
Maceria structure
Paleoenvironment
Furongian
North China Platform

ABSTRACT

This study focuses on the unique occurrence of an extensive microbialite bed (10–20 m thick) in the Chaomidian Formation (Furongian) in Shandong Province, China in order to understand its paleoenvironmental implications. The microbialite bed can be traced for over 6000 km^2 in area. The microbialites are characterized by centimeter- to decimeter-scale branching maze-like constituents (maceriae) of microbial and muddy sediments with chaotic texture, including tabular maceriate microbialite (type 1), columnar maceriate microbialite (type 2), and columnar chaotic microbialite (type 3). Within the bed, each microbialite unit is generally well correlated for tens of kilometers. The entire bed is bounded by limestone–marlstone alternation at the base, and an erosional surface at the top that is subsequently overlain by a grainstone bed of various thicknesses. The microbialite bed formed when the seafloor reached suitable water depth for the microbial growth during sea-level rise accompanied with carbonate production. The maze-like maceria structures formed to acquire a larger surface area under a relatively large input of lime mud. The tabular maceriate microbialites initially formed in relatively deep-water environments and flourished on broad and flat seafloor, whereas the columnar microbialites (types 2 and 3) developed under the influence of strong waves and currents. The microbialite bed was eroded and terminated by frequent storm events and buried under the reworked grainstone. Further rise in sea level and increased metazoan activities afterwards limited the resurgence of microbes in the late Furongian.

1. Introduction

Microbialites are organosedimentary deposits formed by benthic microbial communities which trap detrital sediments and/or induce mineral precipitation (Burne and Moore, 1987; Riding, 2000). Microbialites prevailed in the Middle Cambrian to Furongian after the extinction of archaeocyatha and dwindled in the Ordovician with the appearance of corals, sponges, and stromatoporoids (Riding and Liang, 2005; Riding, 2006). In the North China Platform, deposition of microbialites initiated in the middle Early Cambrian (Zhushadong and Mantou formations) and prevailed during the middle to late Middle Cambrian (Zhangxia Formation) (Chough et al., 2010). After the platform drowning in the late Middle Cambrian (Gushan Formation), microbialites significantly dwindled (Chough et al., 2010).

The primary purpose of this study is to describe a thick biostromal microbialite bed (10–20 m thick) with branching maze-like structures (maceriae) in the middle part of the Chaomidian Formation (Furongian), Shandong Province, China (Fig. 1). The bed can be traced over 100 km, about 6000 km^2 in area. This microbialite bed is unique, because it extensively occurs in the middle of the dwindling stage of microbial growth after the platform drowning. How did microbes thrive on the seafloor during continued rise in sea level? What caused the termination of the microbialite without significant resurgence? How did the maceria structures originate? In order to answer these questions, the present study focuses on the characteristics of the microbialite internal structures and the associated sedimentary facies in well-exposed outcrop sections in Shandong Province.

2. Geological setting

The North China Platform formed on a stable craton, the Sino-Korean Block. It comprises an extensive area of ~1500 km east–west and ~1000 km north–south (Meyerhoff et al., 1991) (Fig. 1A). The western boundary of the platform is characterized by a thick sequence of platform-margin and deep-basinal sediments. The northern, southern, and eastern margins are bounded by major folds and suture zones (the Hinggan fold belt, the Dabieshan belt, and the Tanlu fault, respectively) (Fig. 1A). Sedimentation in the North China Platform initiated in the Early Cambrian and lasted until the Early Ordovician, when the entire platform was subaerially exposed (Meyerhoff et al., 1991; Meng et al., 1997).

* Corresponding author.
E-mail address: sedlab@snu.ac.kr (S.K. Chough).

0031-0182/$ – see front matter © 2010 Elsevier B.V. All rights reserved.
doi:10.1016/j.palaeo.2010.09.012

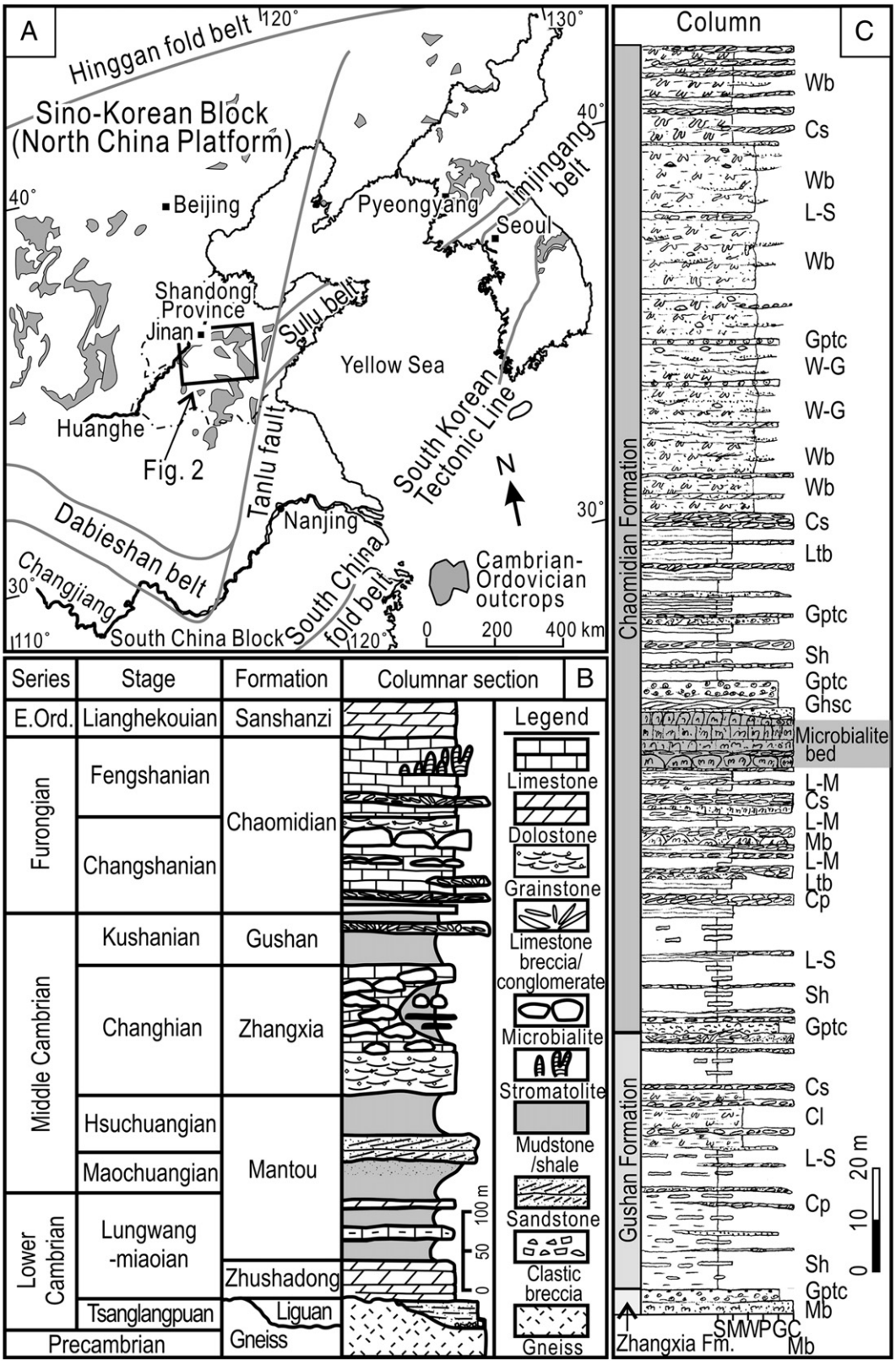

Fig. 1. (A) Distribution of the Cambrian and Ordovician outcrops and major tectonic boundaries in the North China Platform. (B) Summary of the Cambrian stratigraphy in Shandong Province (Modified after Chough et al., 2010). (C) Representative columnar description of the Gushan and Chaomidian formations in the Tangwangzhai section (TWZ). Note the microbialite bed in the middle part of the Chaomidian Formation. For the description of sedimentary facies, see Table 1. S: Shale; M: mudstone; W: wackestone; P: packstone; G: grainstone; C: conglomerate; and Mb: microbialite.

The Cambrian succession in Shandong Province, China consists of six lithostratigraphic units: Liguan, Zhushadong, Mantou, Zhangxia, Gushan, and Chaomidian formations in ascending order (Fig. 1B). The Liguan Formation (20–40 m thick) consists of quartzite and mudstone, unconformably overlying Precambrian granite or sedimentary rocks. The Zhushadong Formation (~30 m thick) consists of wavy and

lenticular laminated dolostone. The overlying Mantou Formation (~200 m thick) is characterized by homogeneous or laminated purple mudstone and cross-laminated purple siltstone. The Zhangxia Formation (~200 m thick) is characterized by thick-bedded limestone including oolitic or oncolitic grainstone, bioturbated lime mudstone, and microbialite. The Gushan Formation (~55 m thick) is composed of shale, lime mudstone, and limestone conglomerate (Meng et al., 1997; Chough et al., 2010).

The Chaomidian Formation, overlying the shale-dominated facies (Gushan Formation), consists mainly of carbonate facies such as limestone–shale alternation (facies L–S), limestone–marlstone alternation (facies L–M), thin-bedded lime mudstone (facies Ltb), limestone conglomerate (facies Cs and Cp), gravelly grainstone (facies Gg), and cross-stratified grainstone (facies Gptc and Ghsc) as well as microbialite (Chen et al., 2009) (Table 1). The microbialite bed (10–20 m thick) occurs in the middle part of the Chaomidian Formation, overlain by a grainstone bed (Fig. 1C). The upper part of the Chaomidian Formation is dominated by wackestone facies (facies Wb and W-G) (Table 1). The Chaomidian Formation formed during the Furongian Changshanian (*Chuangia*, *Changshania–Irvingella*, and *Kaolishania* trilobite biozones) and Fengshanian (*Ptychaspis–Tsinania*, *Quadraticephalus*, and *Mictosaukia* trilobite biozones) stages (Chough et al., 2010).

3. Methods

The microbialite bed occurs as a cliff in many sections. Eight sections in Jinan (Chengouwan, Tangwangzhai, Wanglaoding, Laopozhuang, Wanliangyu, and Duozhuang sections), Taian (Fenghuangshan section), and Laiwu (Jiulongshan section) areas were selected for a detailed description of the microbialite bed (Fig. 2). The microbialites were studied by the four scales of microbialite investigation (i.e., mega-, macro-, meso-, and microscale) (Shapiro, 2000). Line drawings of outcrop sections were made in the field and laboratory to portray the macro- and mesostructures of the microbialites. The microbialite samples were cut and polished for slabs and thin sections in the laboratory. The textual constituents (intermicrobial sediments, calcified microbes, and cements) of the microbialite were determined by using more than 30 polished slabs and about 200 thin sections (Fig. 3).

4. Microbialite bed

4.1. Microbialite types

The microbialites in the Chaomidian Formation clearly show macroscale structures such as columnar structures (Fig. 3D, E). On the

Table 1
Description and interpretation of sedimentary facies.

Sedimentary facies	Description	Interpretation
Shale (facies Sh)	Greenish gray shale; shale mainly composed of quartz and clay minerals, and some calcite and dolomite, partly with nodular limestone; nodular limestone in 1–3 cm thickness, composed of micrite.	Low-energy subtidal deposit most likely below storm wave base (Markello and Read, 1981; Osleger and Read, 1991).
Limestone–shale alternation (facies L–S)	Alternation of limestone and greenish gray shale layers; planar to nodular shaped limestone layers, 1–3 cm thick; less than 1 cm thick shale layers; fine laminations or bioturbations occur in limestone; limestone composed of micrite; shale composed of quartz and clay minerals.	Low-energy subtidal deposit below normal wave base (Kwon et al., 2002; Kwon and Chough, 2005).
Limestone–marlstone alternation (facies L–M)	Alternation of limestone and marlstone layers; limestone layers about 1–2 cm thick, partly bioturbated, composed of micrite and few bioclasts; marlstone layers about 1–10 mm thick, partly crude laminated, composed of dolomite, calcite, and argillaceous grains.	Low-energy subtidal deposit below normal wave base (Markello and Read, 1981; Moshier, 1986; Keller, 1997).
Laminated calcisiltite (facies Cl)	Parallel, ripple, and low-angle cross-laminated calcisiltite intercalated with dolomitic marlstone or shale; composed of silt-sized calcite particles; wavy-bedded, unidirectional, and low-angle cross-lamination with truncational boundary; climbing ripples; partly bioturbated with burrows cutting laminae.	Subtidal deposits by unidirectional currents or combined flows (Kwon et al., 2006; Woo and Chough, 2007).
Thin-bedded lime mudstone (facies Ltb)	Thin-bedded lime mudstone, 1~5 cm thick; sometimes separated by ~1 mm thick marlstone layers; thickness of lime mudstone varies within the same bed, planar to nodular shape; partly bioturbated.	Low-energy subtidal deposit below normal wave base, modified by bioturbation (Calvet and Tucker, 1988).
Hummocky and swaley cross-stratified grainstone (facies Ghsc)	Peloidal grainstone, composed of coarse silt- to very fine sand-grade peloids and small fraction of fossil fragments; Ghsc bed is either laterally continuous or discontinuous, varying in thickness from a few cm to 2 m; variation in thickness of laminae.	Storm deposit by combined flow (Allen, 1985; Myrow and Southard, 1996).
Planar and trough cross-stratified grainstone (facies Gptc)	Planar cross-stratified grainstone with angular or tangential contact with bottom set; partly trough cross-stratified; composed of bioclasts (trilobite and microbial fragments) and ooids.	Subaqueous 2-D or 3-D dune (Moshier, 1986; Strasser, 1986; Myrow et al., 2004).
Gravelly grainstone (facies Gg)	Massive or normally graded gravelly packstone to grainstone; composed of bioclasts (trilobite, brachiopod, algae, echinoderm, and cephalopod; a few mm up to 10 mm in length) and peloids (0.2~0.5 mm in diameter); subangular granules and pebbles of lime mudstone to grainstone commonly at base.	Moderately agitated shallow subtidal deposits (Glumac and Walker, 2000; Woo and Chough, 2007).
Stratified limestone conglomerate (facies Cs)	Granule- to pebble-grade lime mudstone clasts; subrounded to rounded clasts; bioclastic and peloidal grainstone matrix; mostly matrix-supported and partly clast-supported; normally graded or cross-stratified; capped by thin ripple cross-stratified peloidal grainstone.	Deposits by strong currents or waves induced by storms (Walker and Plint, 1992; Demicco and Hardie, 1994).
Limestone pseudoconglomerate (facies Cp)	Laminated or homogeneous lime mudstone clasts; marlstone or peloidal grainstone matrix; clast supported; subrounded to rounded, pebble-grade and flat clasts; partly discontinuous and changing into limestone–shale/marlstone alternation or thin-bedded lime mudstone laterally.	Formed by differential cementation and deformation during early diagenesis (Chough et al., 2001; Chen et al., 2009).
Bioturbated wackestone (facies Wb)	Moderately to severely bioturbated; horizontal to inclined burrows; mottled texture; composed mainly of micrite and fossil fragments and peloids; partly intercalated with thin bioclastic grainstone with sharp lower boundary.	Low-energy subtidal deposit modified by bioturbation (Overstreet et al., 2003).
Wackestone to grainstone (facies W–G)	Flaser-bedded wackestone separated by shale partings; slightly bioturbated; often intercalated with lenses or thin layers of grainstone with sharp lower boundary, partly normally graded or stratified; partly concentrated with cephalopod fossils and shells.	Relatively low-energy subtidal environment with intermittent high-energy conditions (Rees et al., 1976; Nakazawa et al., 2009).

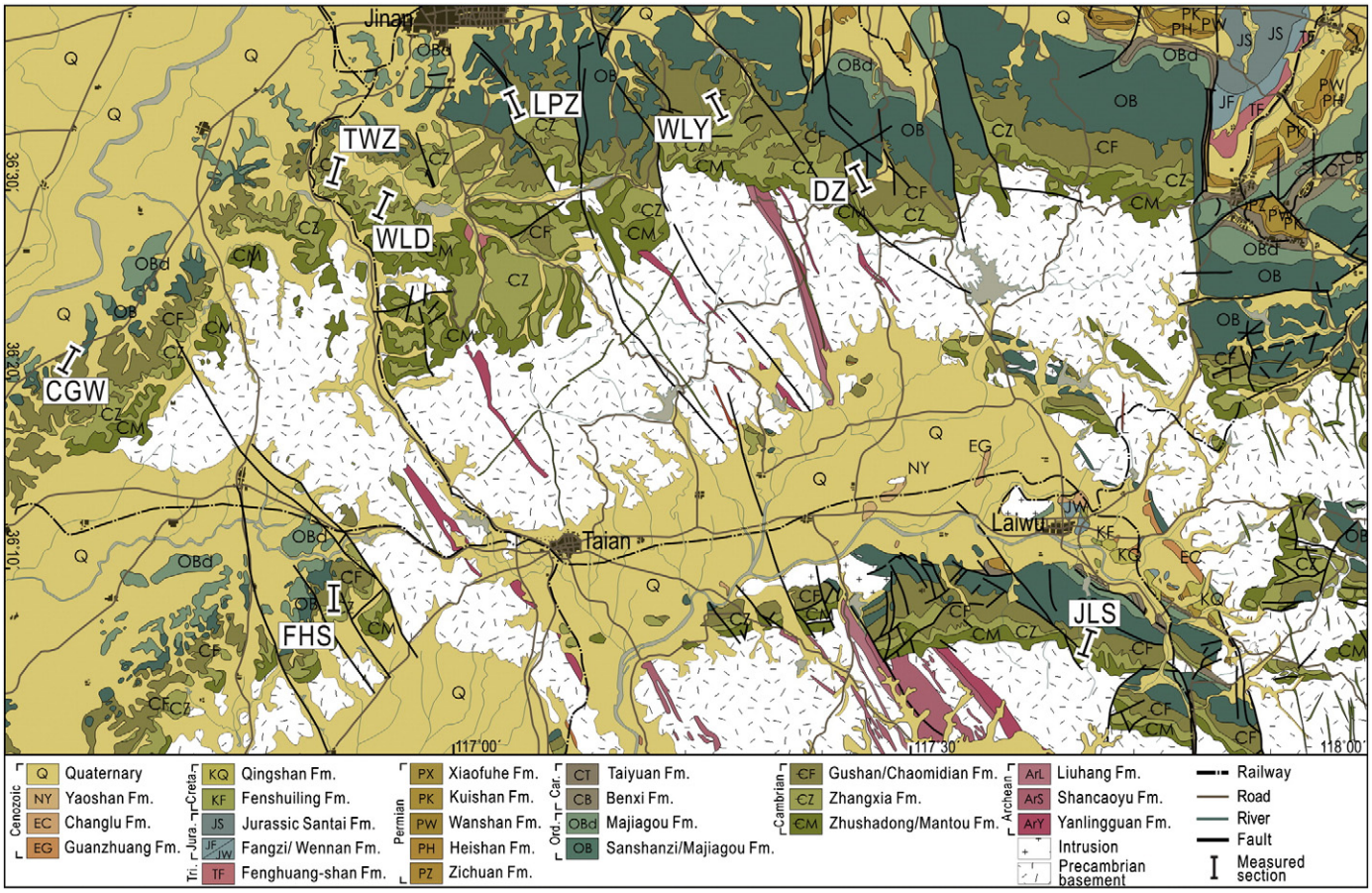

Fig. 2. Geological map and locations of measured sections. CGW: Chengouwan; TWZ: Tangwangzhai; WLD: Wanglaoding; LPZ: Laopozhuang; WLY: Wanliangyu; DZ: Duozhuang; FHS: Fenghuangshan; and JLS: Jiulongshan (Modified after Bureau of Geology and Mineral Resources of Shandong Province, 1996).

contrary, the mesoscale structures of the microbialites are usually chaotic, without clear laminae, clots, or dendroids (Fig. 3F). In microscale, the microbialites are mainly composed of calcified *Girvanella*, detrital sediment, and cement (Fig. 3G). Centimeter- to decimeter-scale branching structures containing chaotic mesostructures occur within macroscale structures (i.e., tabular and columnar structures) (Fig. 4). These branching structures are identified as 'maceriae' (singular: maceria) (Shapiro and Awramik, 2006). The maceriae commonly occur as branching and converging thin ribbons in vertical sections (Fig. 4A, B), and irregular circles or rambling maze-like structures in horizontal sections (Fig. 4C, D). Each maceria is less than 2 cm in width and composed of thin microbialite walls, filled with intermacerial sediments (Fig. 4E). The boundaries between maceriae and intermacerial sediments are ragged and obscure (Fig. 4A). Maceria structures show upward branching and converging trends (Fig. 4E). The maceriate microbialites (microbialite with maceria structures), similar to *Favosamaceria* reported from Cambrian–Ordovician deposits of Laurentia (Shapiro and Awramik, 2006), constitute a major portion of the microbialite bed. Three types of microbialites are classified, i.e., tabular maceriate microbialite (type 1), columnar maceriate microbialite (type 2), and columnar chaotic microbialite (type 3) (Table 2).

4.1.1. Tabular maceriate microbialite (type 1)

The tabular maceriate microbialite is either isolated, forming a bioherm, or connected, forming a biostrome. The former consists of 1–2 m thick and ~10 m wide mound (Fig. 5A), whereas the latter occurs as a single bed. The tabular maceriate microbialites consist of maceria and intermacerial sediment (Fig. 5B). The internal structures of maceriae are usually chaotic in which microbial-origin sediments are not well differentiated from the non-microbial sediments (Fig. 5C). The intermacerial sediment is mainly composed of lime mud and a few bioclasts (mostly trilobites), whereas the maceria is mainly composed of micrite and calcified *Girvanella* (Fig. 5C, D) as well as calcified *Renalcis*-like microbe colonies (1–4 cm in size) (Fig. 5E). The calcified *Renalcis*-like microbes, showing grape-like chambers, are composed of sparite and surrounded by micrite with *Girvanella*, which is different from *Renalcis* that is composed of micrite and surrounded by sparite (Riding, 1991) (Fig. 5F). The tabular maceriate microbialite is often underlain by a bed of limestone–marlstone alternation (facies L–M) or other microbialites with a sharp boundary, and overlain by tabular maceriate microbialite, grainstone (facies Gptc), limestone conglomerate (facies Cs and Cp), or limestone–marlstone alternation (facies L–M).

4.1.2. Columnar maceriate microbialite (type 2)

The columnar maceriate microbialite is represented by a columnar structure (>60 cm in diameter), forming a megascale biostrome (Fig. 6A). The internal part is dominated by maceriae, whereas the outer rim of the column (~10 cm in thickness in horizontal sections) is chaotic (Fig. 6B, C). Lime mud and bioclasts occur as intermacerial sediment and coarse-grained sediments occur in the outer rim of the columns. Intercolumnar sediments are generally composed of coarse-grained sediments such as intraclasts, peloids, and bioclasts, with partially dolomitized sediments. The columnar maceriate microbialite is differentiated from the tabular maceriate microbialite by the occurrence of intercolumnar grainstone and coarse-grained outer rim. The columnar maceriate microbialite changes upward to columnar chaotic microbialite (Fig. 6D), accompanied by a decrease in amounts of maceriae, an increase in amounts of intercolumnar grainstone, and

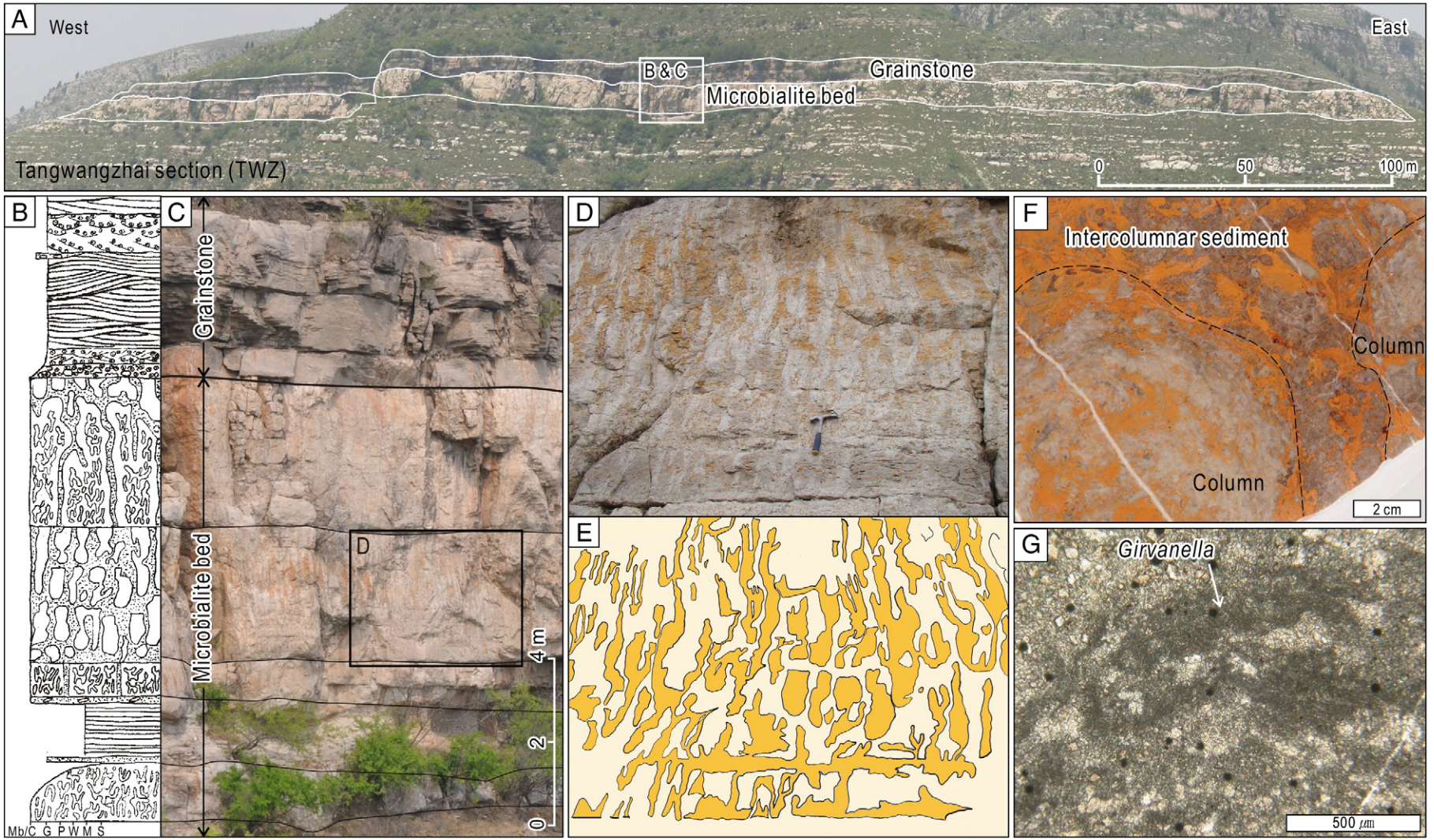

Fig. 3. Representative mega- to microscale structures of the microbialite bed in the Tangwangzhai section. (A) Panoramic outcrop photograph of the microbialite bed and the overlying grainstone bed. Columnar description (B) and close-up view (C), showing the microbialite and grainstone with a distinct boundary. Columnar chaotic microbialites in vertical section (D) and line drawing (E). Hammer is 28 cm in length. (F) Polished slab of columnar chaotic microbialite (horizontal section). (G) Photomicrograph of columnar chaotic microbialite. Calcified *Girvanella* occurs within the micrites.

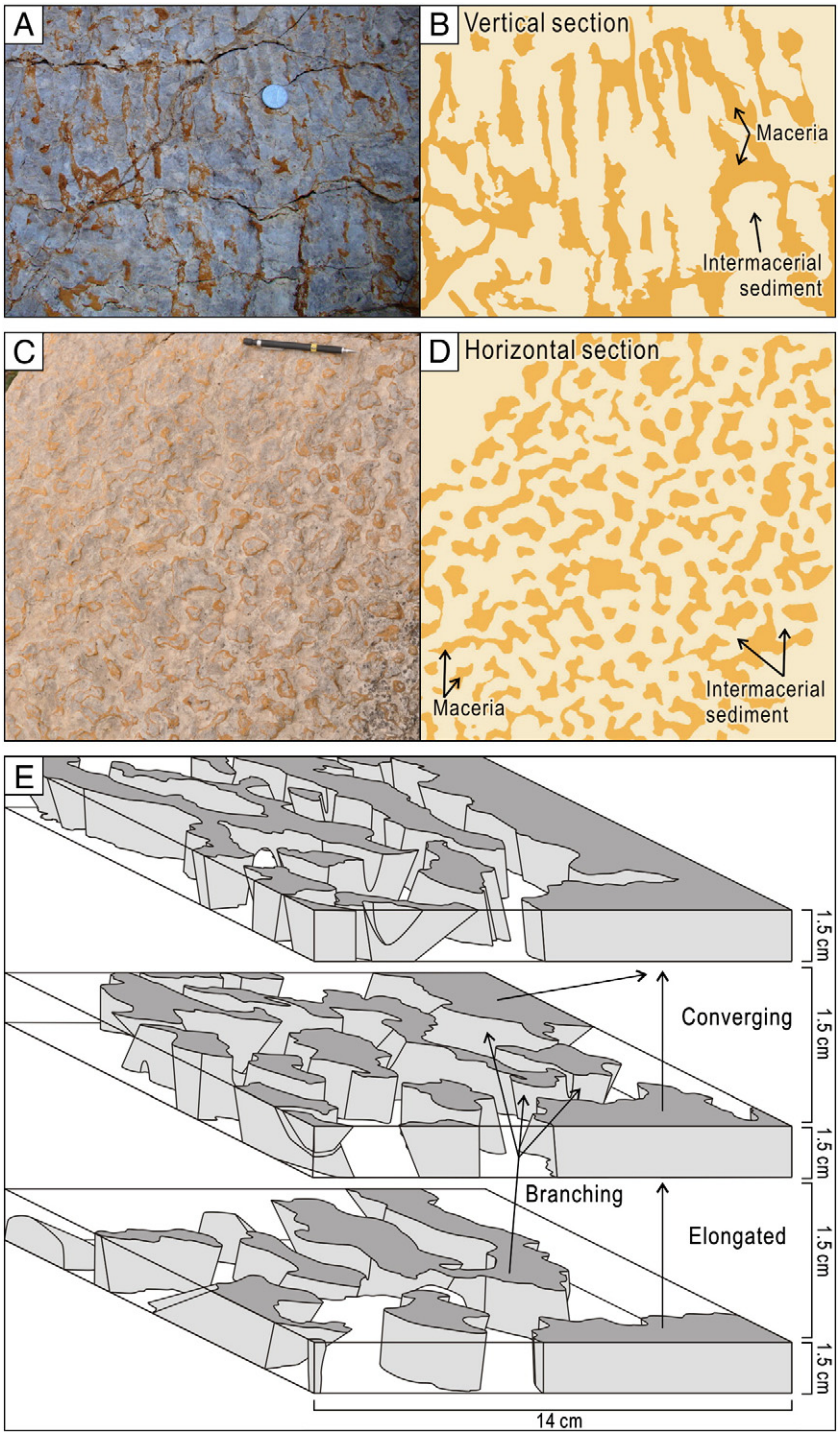

Fig. 4. Photograph (A) and line drawing (B) of thin ribbon-like maceria structures in vertical section (Tangwangzhai section). Coin is 19 mm in diameter. Photograph (C) and line drawing (D) of irregular circles or rambling maze-like maceria structures in horizontal section (Laopozhuang section). Mechanical pencil is 15 cm in length. (E) 3-D reconstruction of maceria structures, showing upward branching or converging patterns. Intermacerial sediments are excluded from the reconstruction.

a decrease in column diameter (i.e., increase in elongation ratio of column).

4.1.3. Columnar chaotic microbialite (type 3)

The columnar chaotic microbialite is represented by a group of columnar structures (10–15 cm in diameter) whose internal structures are generally chaotic (Fig. 7A, B, and C). The boundaries between microbialites and intercolumnar sediments are smooth and clear (Fig. 7C). The elongation aspect ratio (i.e., ratio of height to width) of columns ranges from 3:1 to 10:1. Calcified *Girvanella* occurs in microscale with micrite, sparite, peloid, bioclast, and *Renalcis*-like microbes similar to those of the tabular microbialite (Fig. 7D). Crudely stratified grainstones among the microbialite columns consist of peloids and microbialite clasts of *Girvanella* fragments. Fossils of benthic organisms (e.g., trilobite, brachiopod, and bivalve) occur in both intercolumnar sediments and microbialites. The columnar chaotic microbialite is overlain by either microbialite (tabular maceriate and columnar maceriate microbialites) or grainstone with a sharp erosional boundary.

Table 2
Description and interpretation of microbialites.

Microbialite types	Macro-structures	Internal structures	Diagram	Description	Interpretation
Tabular maceriate microbialite (type 1)	Tabular	Maceria and chaotic	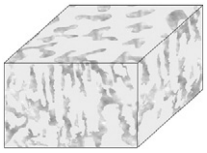	Biohermal/biostromal megastructure (Fig. 5A); consists of maceriae and intermacerial sediment with a ragged, obscure boundary (Fig. 5B); internal structure of maceriae are chaotic (Fig. 5C); intermacerial sediments composed of lime mud and bioclasts; maceriae composed of micrite, *Girvanella*, and *Renalcis*-like microbe (Fig. 5D, E, and F).	Low-energy environments below normal wave base.
Columnar maceriate microbialite (type 2)	Columnar	Maceria and chaotic	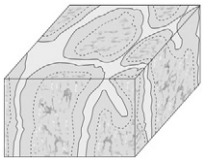	Columnar structure (>60 cm) within biostrome (Fig. 6A); maceriae occur as internal structure, with chaotic outer rim (Fig. 6B, C); coarse-grained intercolumnar sediments; type 2 microbialite changes upward to type 3 (Fig. 6D).	Intermediate-energy environments near normal wave base.
Columnar chaotic microbialite (type 3)	Columnar	Chaotic	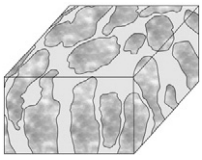	Columnar structure (10–15 cm in diameter) (Fig. 7A, B, and C); elongation ratio of columns ranges from 3:1 to 10:1; smooth, clear boundary; micrite, sparite, peloid, bioclast, *Girvanella* and *Renalcis*-like microbe in microscale (Fig. 7D); intercolumnar sediments consist of peloids and microbialite clasts of *Girvanella* fragments.	High-energy shallow environments above normal wave base.

4.2. Description of microbialite bed and grainstone bed

In eight measured sections, the tabular maceriate microbialite (type 1) occurs in the lowermost part of the bed, overlying the limestone and marlstone alternation. In the western area (Chengouwan, Fenghuangshan, Tangwangzhai, Wanglaoding, and Laopozhuang sections), individual units of columnar microbialites (types 2 and 3) with sharp boundaries are well correlated for tens of kilometers, whereas in the eastern area (Wanliangyu and Duozhuang sections), tabular maceriate microbialites (type 1) are dominant throughout the bed (Fig. 8). The Jiulongshan section is dominated by biostromal tabular maceriate microbialite interbedded with limestone–marlstone alternation, limestone conglomerates, and planar and trough cross-stratified grainstone.

A grainstone bed of various thicknesses (2.5–16.5 m) overlies the entire microbialite bed upon an erosional boundary. The overlying grainstone bed consists of hummocky and swaley cross-stratified grainstone, planar and trough cross-stratified grainstone, gravelly grainstone, limestone and marlstone alternation, stratified limestone conglomerate, and limestone pseudoconglomerate (Table 1). The Changshanian–Fengshanian stage boundary (*Ptychaspis–Tsinania* biozone) occurs in the upper part of the grainstone bed (Fig. 8).

5. Discussion

5.1. Depositional processes

The low synoptic relief of the maceriate microbialite during growth (less than half of the maceria width; estimated based on the ragged, obscure boundaries of maceria structures) suggests that the growth rate of microbialite and the background sedimentation rate were similar (James and Bourque, 1992; Shapiro and Awramik, 2006). The occurrence of abundant lime mud as intermacerial sediments indicates low-energy environments. The maceriae-dominated microbialites (i.e., tabular maceriate and columnar maceriate microbialites; types 1 and 2) were most likely deposited under low-energy conditions, either below or above normal wave base. The lack of exposure structures in the microbialite bed is, however, suggestive of deposition in relatively deep-water, low-energy environments (Fig. 9A, B).

Smooth and clear boundaries between columnar microbialites and intercolumnar sediments are suggested of higher synoptic relief of columnar microbialites during growth than that of the maceriate microbialites (James and Bourque, 1992). The columnar microbialites are interpreted as the deposit of subtidal environments (Griffin, 1989; Shapiro, 1995; Rowland and Shapiro, 2002). The high elongation aspect ratio (3:1–10:1) of the columnar structures is indicative of high-energy level (Grotzinger, 1989). Coarse-grained sediments both in the microbialite and among the columns are also indicative of high-energy conditions. Therefore, the columnar chaotic microbialite (type 3) was most likely deposited above normal wave base, where strong waves and currents dominated (Fig. 9B).

The columnar maceriate microbialite (type 2) contains characteristics of both tabular maceriate microbialite (type 1) and columnar chaotic microbialite (type 3), suggesting deposition near normal wave base where strong waves and currents occasionally occur. A decrease in amounts of maceriae, an increase in amounts of intercolumnar coarse-grained sediment, and an increase in elongation aspect ratio of columnar structures collectively suggest that the gradual change from the columnar maceriate microbialite (type 2) to columnar chaotic microbialite (type 3) probably resulted from a gradual increase in energy level (Horodyski, 1977; Grotzinger, 1989) (Fig. 6D).

5.2. Flourish and demise

The shallow and broad North China Platform was located in low latitudes during the Cambrian period (Scotese and McKerrow, 1991; Li and Powell, 2001), and could have provided favorable conditions (e.g., warm and clear sea water, enough sunlight, etc.) for the flourish of microbialites (Burne and Moore, 1987; Riding, 2000). During the Furongian, the platform gradually formed a broad and relatively flat seafloor with an interaction of relative sea-level rise, and carbonate production and sedimentation (Meng et al., 1997). The extensive area of the North China Platform might have reached suitable water depths for microbial growth when carbonate production eventually caught up and kept up with relative sea-level rise after platform drowning. The microbialite might have developed contemporaneously on the broad and relatively flat seafloor, mainly because individual units within the microbialite bed, composed of similar internal structures and bounded by sharp erosional boundaries, can be laterally traced for

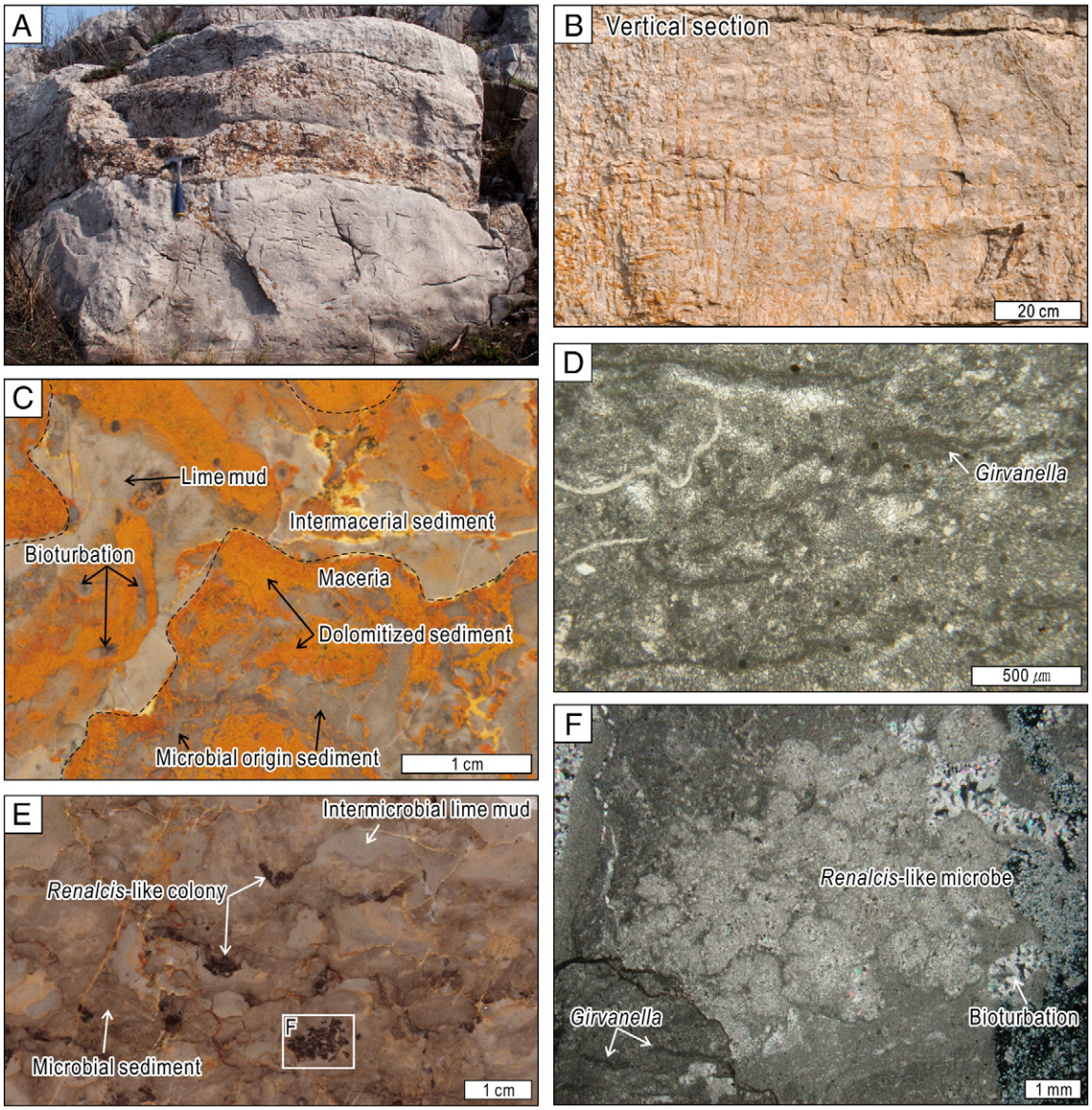

Fig. 5. (A) Photograph of tabular maceriate microbialite (type 1) (biohermal megastructures) (Jiulongshan section). Hammer is 28 cm in length. (B) Close-up view of tabular maceriate microbialite in vertical section (Laopozhuang section). (C) Polished slab of maceria structures in horizontal section (Tangwangzhai section). Maceria structures consist of microbial-origin sediment and dolomitized sediment. Internal structures of maceriae are chaotic. Intermacerial sediment consists of bioturbated lime mud and dolomite. (D) Photomicrograph of calcified *Girvanella* and micrite. (E) Colony of *Renalcis*-like microbes occurs in dark brown color with light gray intermicrobial lime mud and gray microbial sediment. (F) Photomicrograph of *Renalcis*-like microbes which consist of sparites, surrounded by micrites. Calcified *Girvanella* occurs within the surrounding micrites.

tens of kilometers (Fig. 8). The deposition of the tabular maceriate microbialites (type 1) initiated most likely under relatively deep-water environments (Fig. 9A). Due to different hydraulic conditions, sedimentation rates, and growth rates of microbialites, the tabular maceriate microbialites (type 1) developed dominantly in the eastern area, whereas the columnar microbialites (types 2 and 3) in the western area (Fig. 9B).

The termination of microbialites was most likely induced by frequent storms, which eroded the uppermost part of the microbialite bed by waves and currents (cf. Adams et al., 2005). Microbialites were subsequently buried by reworked sediments. The storm-induced sedimentary facies (i.e., hummocky cross-stratified grainstone and stratified conglomerate) in the overlying grainstone bed indicates that the termination processes occurred above storm wave base (Fig. 9C). After the termination of the microbialites, the North China Platform was drowned again with rise in sea level during the Furongian, which restricted the growth of microbes by limiting sunlight penetration. As the water depth was shallowed again during the late Furongian (upper part of the Chaomidian Formation), the metazoan activities (including grazing and burrowing) increased significantly with limited resurgence of the microbialites (Garrett, 1970; Gischler et al., 2008).

5.3. Origin of the maceria structures

Previous studies indicate that the maceriate microbialites are limited to a short period from the Furongian to Early Ordovician in Laurentia (Shapiro and Awramik, 2006). Based on the time-limited occurrence of maceriate microbialites and their appearance in various depositional environments, Shapiro and Awramik (2006) have suggested that the biological control on maceria structures is more important than the environmental control; this indicates that a specific microbial taxon or a group of taxa, responsible for maceria structures, might have occurred in this period. However, no microbial

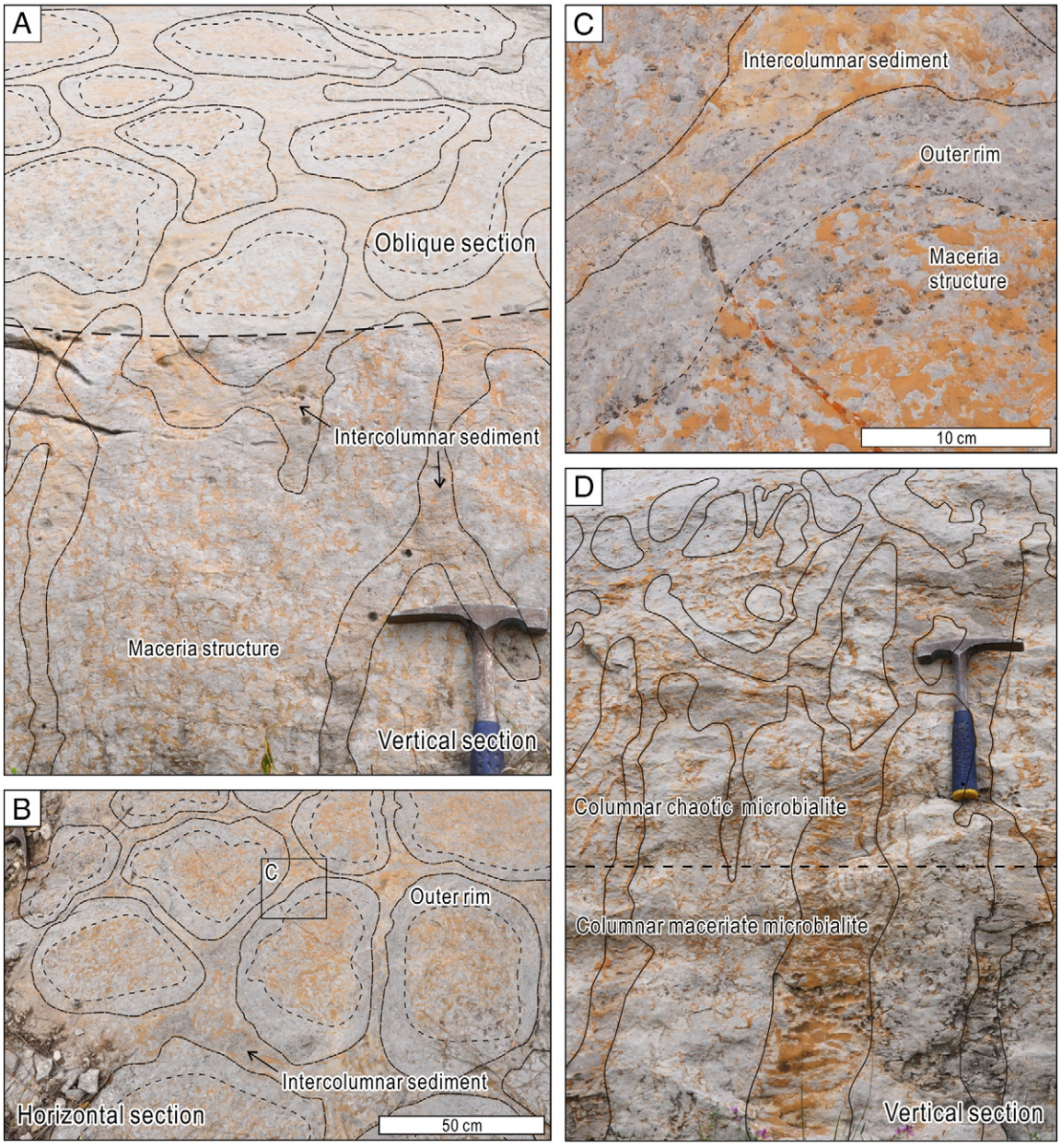

Fig. 6. (A) Columnar maceriate microbialite (type 2) in vertical and oblique sections (Chengouwan section). Hammer is 28 cm in length. (B) In horizontal section, it consists of maceriae in the inner part and coarse-grained microbialites in the outer rim. (C) Close-up view in horizontal section. (D) An upward gradual change from columnar maceriate microbialite to columnar chaotic microbialite. Hammer is 28 cm in length.

taxon has been reported from the maceriate microbialites due to the obscure microstructures (e.g., Mazzullo and Friedman, 1977; Armella, 1994; Shapiro and Awramik, 2006). Instead, a unique combination of global environmental factors (i.e., sea-water chemistry, carbonate production, and lack of metazoan reef builders) of the Furongian to Early Ordovician might have been critical to the formation of maceria structures.

Significant global warming during the Cambrian resulted in both a long-term eustatic rise in sea level and an extensive development of shallow epeiric seas (Prothero and Dott, 2009). Sea-water chemistry changed with the progression of the greenhouse period and the prolonged sea-level rise, from an aragonite-precipitating phase into a calcite-precipitating phase (Sandberg, 1983; Zhuravlev and Wood, 2008). This resulted in rapid marine cementation of carbonate sediments and enhanced precipitation of microcrystalline carbonate and calcification of microbial organisms (Wilson and Palmer, 1992). On the other hand, the lack of reef-building metazoan communities after mass extinction in the late Early Cambrian (Zhuravlev, 1996; Zhuravlev and Wood, 1996) gave rise to flourishing of microbial organisms in reef communities (Sepkoski, 1996; Erwin, 1998). The calcified cyanobacterial filaments (e.g., *Girvanella*) might have provided abundant lime mud in the lower Paleozoic (Pratt, 2001). Therefore, the sedimentation rate of lime mud during the Furongian to Early Ordovician would have been relatively higher than other periods in Phanerozoic.

Shapiro and Awramik (2006) assumed that the synoptic relief of maceria structures above the sediment surface would have been less than 5 mm, based on the maceria–intermacerial sediment relationships. This indicates that the growth rate of microbialites would have been balanced with the sedimentation rate of lime mud. Under this condition, the microbialites could not have formed smooth top surfaces which could be easily covered by lime mud. Instead, the

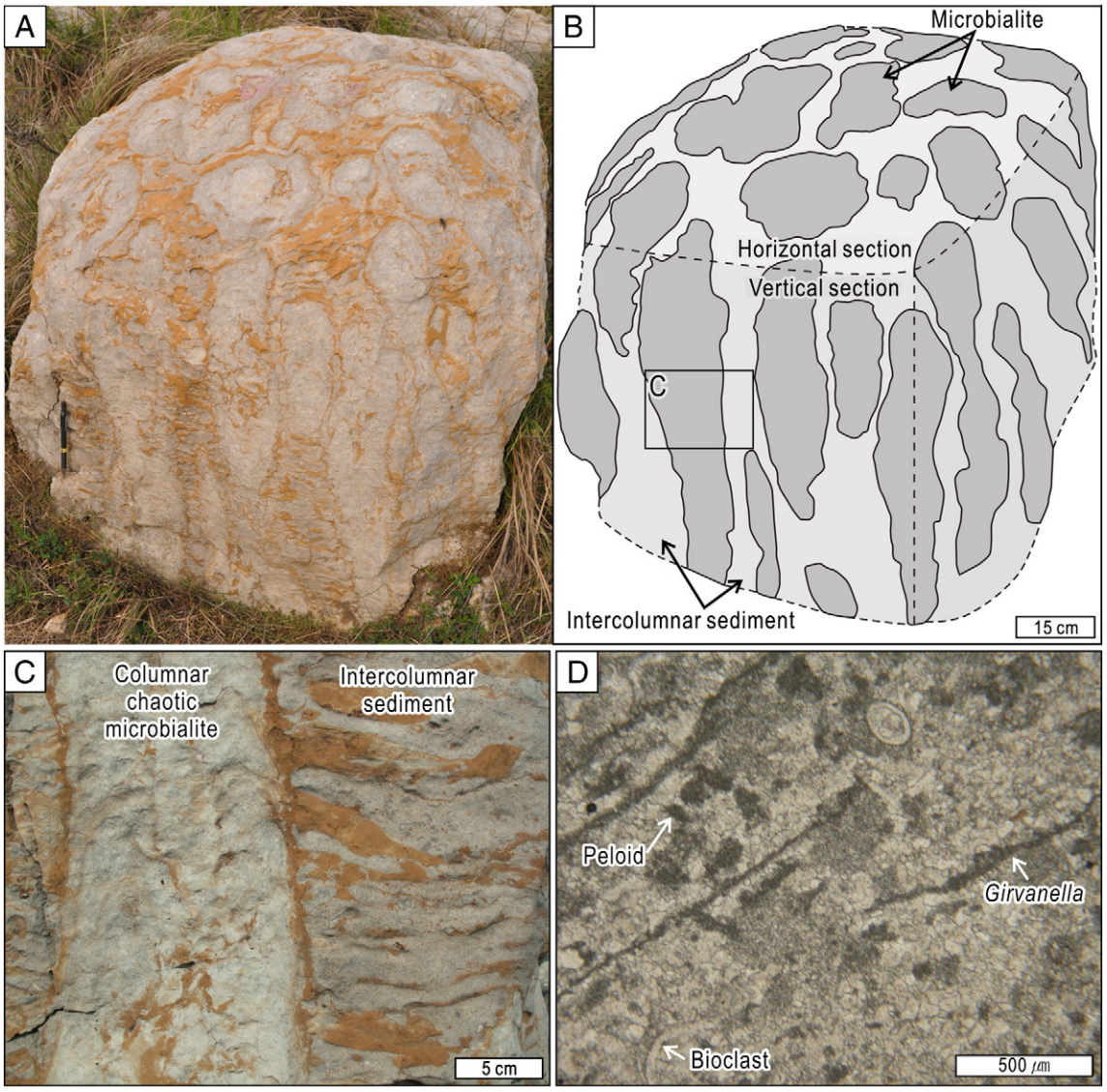

Fig. 7. Photograph (A) and line drawing (B) of columnar chaotic microbialites (type 3) (Tangwangzhai section). (C) Close-up view in vertical section. (D) Calcified microbe *Girvanella* in thin section.

microbialites formed the maze-like structures to be not covered by lime mud. The top surface of microbialites in the initiation stage might have been uneven, at least in mesoscale. The uneven surface would have resulted in partially different conditions; lime mud would have deposited in the lower area of the uneven surface, which would have enforced microbialites to grow on the higher area of the uneven surface. With continued sedimentation of lime mud, microbialites would have formed maze-like complex structures.

The maze-like complex structures commonly occur in nature from mitochondria to intestine of animals. These complex structures usually form to acquire a larger surface area within a limited volume. Microbialites also increased their surface area during growth in order to acquire enough surface area to receive sunlight and nutrients (Horodyski, 1977; Awramik and Vanyo, 1986). The microbialites form various structures such as dome, column, or upward-widening fan shape in order to increase surface area if synoptic relief during growth is high enough (e.g., Grotzinger and Knoll, 1999; Riding, 2000; Woo and Chough, 2010). If the microbialites formed a simple shape such as columnar structures when the growth rate of microbialites was balanced with background sedimentation rate, the top surface area to volume ratio would have been smaller than that of the complex maze-like structures if the volume is similar. The maze-like structures of maceriate microbialite would have provided them enough surface area to acquire sunlight and nutrients.

6. Conclusions

1. Three types of microbialites occur in the microbialite bed of the Furongian Chaomidian Formation, Shandong Province, China. These microbialites are characterized by maze-like maceria structures and chaotic mesostructures. The tabular maceriate microbialites (type 1) formed in relatively deep-water environments, whereas the columnar microbialites (types 2 and 3) formed under the effects of strong waves and currents.
2. The microbialite bed initiated and flourished as sea level rose and carbonate production progressively increased when the seafloor reached suitable water depth for the microbial growth. It was terminated by extensive erosion and subsequent deposition of reworked grainstone induced by storm events. Both further rapid rise in sea level and increased metazoan activities limited significant resurgence of microbialites.
3. The maceria structures (maceriate microbialite) formed when the growth rate of microbialites was balanced with the sedimentation rate of lime mud.

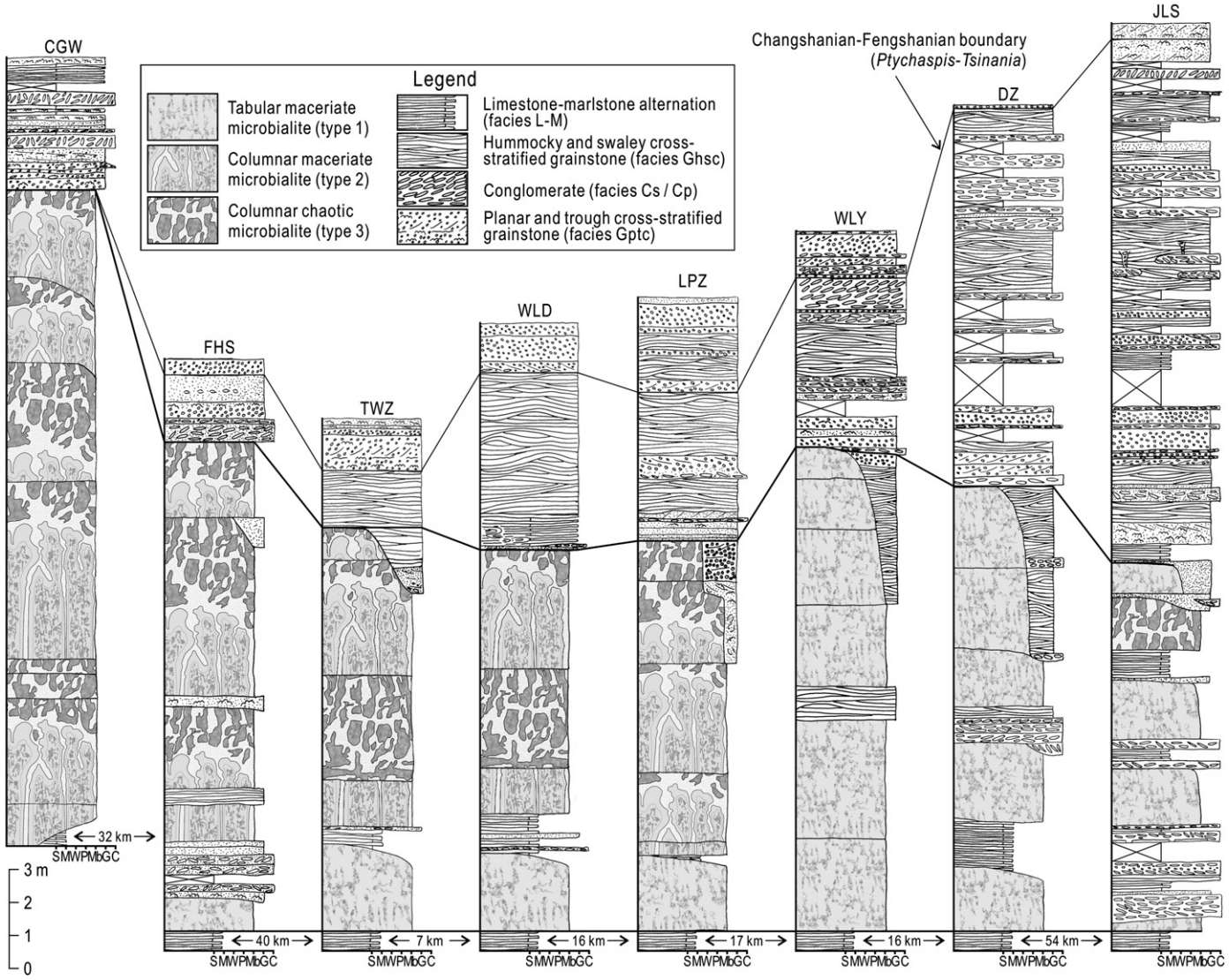

Fig. 8. Columnar description and correlation of the microbialite bed in eight sections. For the location of the sections, see Fig. 2. The lower and upper boundaries of the microbialite bed are indicated by thick line. The Changshanian–Fengshanian stage boundary occurs in the upper part of the grainstone bed. S: Shale; M: mudstone; W: wackestone; P: packstone; Mb: microbialite; G: grainstone; and C: conglomerate.

Acknowledgements

This study was supported by grants to Chough by the National Research Foundation (2009-0093871) and the BK 21 project (Ministry of Education and Human Resources). We are grateful to Z. Han for his logistic and the financial support by the National Natural Science Foundation of China (40972043). We acknowledge J. Woo, H.S. Lee, S.-b. Lee, and T.-y. Park for helpful discussions in the field and laboratory. We also appreciate constructive reviews of R. Shapiro and R. Riding.

References

Adams, E.W., Grotzinger, J.P., Watters, W.A., Schröder, S., McCormick, D.S., Al-Siyabi, H.A., 2005. Digital characterization of thrombolite–stromatolite reef distribution in a carbonate ramp system (terminal Proterozoic, Nama Group, Namibia). AAPG Bulletin 89, 1293–1318.

Allen, P.A., 1985. Hummocky cross-stratification is not produced purely under progressive gravity waves. Nature 313, 562–564.

Armella, C., 1994. Thrombolitic–stromatolitic cycles of the Cambro–Ordovician boundary sequence, Precordillera Oriental basin, western Argentina. In: Bertrand-Sarfati, J., Monty, C.L.V. (Eds.), Phanerozoic Stromatolites II. Kluwer Academic, Dordrecht, Netherlands, pp. 421–441.

Awramik, S.M., Vanyo, J.P., 1986. Heliotropism in modern stromatolites. Science 231, 1279–1281.

Bureau of Geology and Mineral Resources of Shandong Province, 1996. Stratigraphy (Lithostratigraphy) of Shandong Province. China University of Geoscience Press, Beijing, China. (328 pp., In Chinese).

Burne, R.V., Moore, L.S., 1987. Microbialites: organosedimentary deposits of benthic microbial communities. Palaios 2, 241–254.

Calvet, F., Tucker, M.E., 1988. Outer ramp cycles in the Upper Muschelkalk of the Catalan Basin, northeast Spain. Sedimentary Geology 57, 185–198.

Chen, J., Chough, S.K., Chun, S.S., Han, Z., 2009. Limestone pseudoconglomerates in the Late Cambrian Gushan and Chaomidian formations (Shandong Province, China): soft-sediment deformation induced by storm-wave loading. Sedimentology 56, 1174–1195.

Chough, S.K., Kwon, Y.K., Choi, D.K., Lee, D.J., 2001. Autoconglomeration of limestone. Geosciences Journal 5, 159–164.

Chough, S.K., Lee, H.S., Woo, J., Chen, J., Choi, D.K., Lee, S.-B., Kang, I., Park, T.-Y., Han, Z., 2010. Cambrian stratigraphy of the North China Platform: revisiting principal sections in Shandong Province, China. Geosciences Journal 14, 235–268.

Demicco, R.V., Hardie, L.A., 1994. Sedimentary structures and early diagenetic features of shallow marine carbonate deposits: SEPM Atlas Series 1, Tulsa, Oklahoma (265 pp.).

Erwin, D.H., 1998. The end and the beginning: recoveries from mass extinctions. Trends in Ecology and Evolution 13, 344–349.

Garrett, P., 1970. Phanerozoic stromatolites: noncompetitive ecologic restriction by grazing and burrowing animals. Science 169, 171–173.

Gischler, E., Gibson, M.A., Oschmann, W., 2008. Giant Holocene freshwater microbialites, Laguna Bacalar, Quintana Roo, Mexico. Sedimentology 55, 1293–1309.

Glumac, B., Walker, K.R., 2000. Carbonate deposition and sequence stratigraphy of the terminal Cambrian grand cycle in the Southern Appalachians, U.S.A. Journal of Sedimentary Research 70, 952–963.

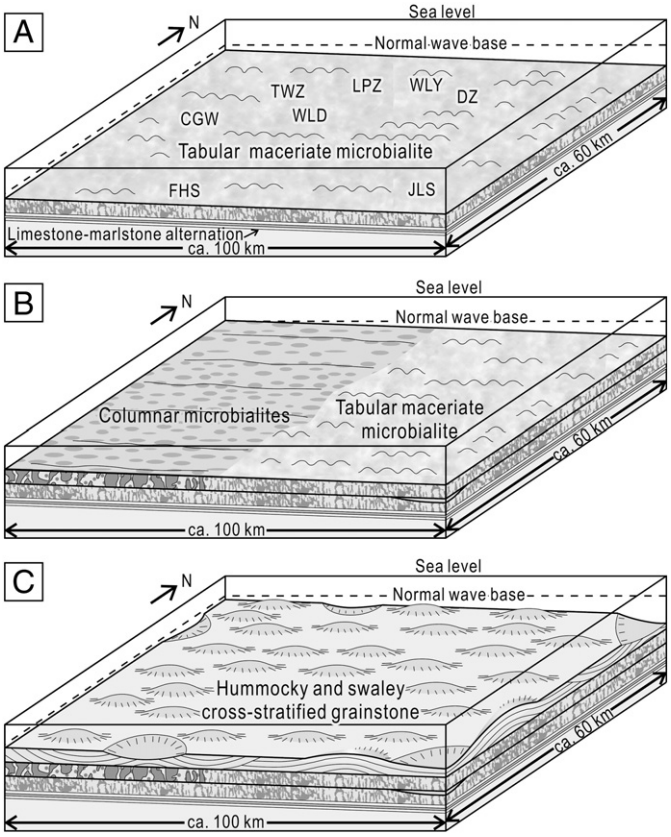

Fig. 9. Depositional model. (A) The early stage was dominated by tabular maceriate microbialites (type 1), in relatively deep-water environments. (B) During the middle to late stage, the eastern seafloor continued to stay in relatively deep-water environments, dominated by tabular maceriate microbialites (type 1). The western seafloor was affected by strong wave and currents, forming the columnar microbialites (types 2 and 3). (C) The microbialite bed was terminated by storm-induced extensive erosion followed by the deposition of grainstone. CGW: Chengouwan; TWZ: Tangwangzhai; WLD: Wanglaoding; LPZ: Laopozhuang; WLY: Wanliangyu; DZ: Duozhuang; FHS: Fenghuangshan; and JLS: Jiulongshan.

Griffin, K.M., 1989. In: Cooper, J.D. (Ed.), Microbial reefs on a carbonate ramp: a case study from western North America with a global perspective. : Cavalcade of Carbonates. Pacific Section Society, pp. 101–112.

Grotzinger, J.P., 1989. Facies and evolution of Precambrian carbonate depositional systems: emergence of the modern platform archetype. In: Crevello, P.D., Wilson, J.L., Sarg, J.F., Read, J.F. (Eds.), Controls on carbonate platform development: SEPM Special Publication, 44, pp. 79–106.

Grotzinger, J.P., Knoll, A.H., 1999. Stromatolites in Precambrian carbonates: evolutionary mileposts or environmental dipsticks? Annual Review of Earth and Planetary Science 27, 313–358.

Horodyski, R.J., 1977. Environmental influences on columnar stromatolite branching patterns: examples from the Middle Proterozoic belt supergroup, Glacier national park, Montana. Journal of Paleontology 51, 661–671.

James, N.P., Bourque, P.-A., 1992. Reefs and mounds. In: Walker, R.G., James, N.P. (Eds.), Facies models: response to sea level change: Geological Association of Canada, St. John's, Canada, pp. 323–348.

Keller, M., 1997. Evolution and sequence stratigraphy of an Early Devonian carbonate ramp, Cantabrian Mountains, Northern Spain. Journal of Sedimentary Research 67, 638–652.

Kwon, Y.K., Chough, S.K., 2005. Sequence stratigraphy of the cyclic successions in the Dumugol Formation (Lower Ordovician), mideast Korea. Geosciences Journal 9, 305–324.

Kwon, Y.K., Chough, S.K., Choi, D.K., Lee, D.J., 2002. Origin of limestone conglomerates in the Choson Supergroup (Cambro–Ordovician), mid-east Korea. Sedimentary Geology 146, 265–283.

Kwon, Y.K., Chough, S.K., Choi, D.K., Lee, D.J., 2006. Sequence stratigraphy of the Taebaek Group (Cambrian–Ordovician), mideast Korea. Sedimentary Geology 192, 19–55.

Li, Z.X., Powell, C. McA, 2001. An outline of the palaeogeographic evolution of the Australasian region since the beginning of the Neoproterozoic. Earth-Science Reviews 53, 237–277.

Markello, J.R., Read, J.F., 1981. Carbonate ramp-to-deeper shale shelf transitions of an Upper Cambrian intrashelf basin, Nolichucky Formation, Southwest Virginia Appalachians. Sedimentology 28, 573–597.

Mazzullo, S.J., Friedman, G.M., 1977. Competitive algal colonization of peritidal flats in a schizohaline environment: the Lower Ordovician of New York. Journal of Sedimentary Petrology 47, 398–410.

Meng, X., Ge, M., Tucker, M.E., 1997. Sequence stratigraphy, sea-level changes and depositional systems in the Cambro–Ordovician of the North China carbonate platform. Sedimentary Geology 114, 189–222.

Meyerhoff, A.A., Kamen-Kaye, M., Chen, C., Taner, I., 1991. China—Stratigraphy, Paleogeography, and Tectonics. Kluwer Academic Publishers. (188 pp.).

Moshier, S.O., 1986. Carbonate platform sedimentology, Upper Cambrian Richland Formation, Lebanon Valley, Pennsylvania. Journal of Sedimentary Petrology 56, 204–216.

Myrow, P.M., Southard, J.B., 1996. Tempestite deposition. Journal of Sedimentary Research 66, 875–887.

Myrow, P.M., Tice, L., Archuleta, B., Clark, B., Taylor, J.F., Ripperdan, R.L., 2004. Flat-pebble conglomerate: its multiple origins and relationship to meter-scale depositional cycles. Sedimentology 51, 973–996.

Nakazawa, T., Ueno, K., Kawahata, H., Fujikawa, M., Kashiwagi, K., 2009. Facies stacking patterns in high-frequency sequences influenced by long-term sea-level change on a Permian Panthalassan oceanic atoll: an example from the Akiyoshi Limestone, SW Japan. Sedimentary Geology 214, 35–48.

Osleger, D.A., Read, J.F., 1991. Relation of eustasy to stacking patterns of meter-scale carbonate cycles, Late Cambrian, U.S.A. Journal of Sedimentary Petrology 61, 1225–1252.

Overstreet, R.B., Oboh-Ikuenobe, F.E., Gregg, J.M., 2003. Sequence stratigraphy and depositional facies of Lower Ordovician cyclic carbonate rocks, southern Missouri, U.S.A. Journal of Sedimentary Research 73, 421–433.

Pratt, B.R., 2001. Calcification of cyanobacterial filaments: *Girvanella* and the origin of lower Paleozoic lime mud. Geology 29, 763–766.

Prothero, D.R., Dott, R.H., 2009. Evolution of the Earth, 8th edition. McGraw-Hill. (576 pp.).

Rees, M.N., Brady, M.J., Rowell, A.J., 1976. Depositional environments of the Upper Cambrian John Wash Limestone (House Range, Utah). Journal of Sedimentary Petrology 46, 38–47.

Riding, R., 1991. Calcified cyanobacteria. In: Riding, R. (Ed.), Calcareous Algae and Stromatolites. Springer-Verlag, Berlin, pp. 55–87.

Riding, R., 2000. Microbial carbonates: the geological record of calcified bacterial-algal mats and biofilms. Sedimentology 47, 179–214.

Riding, R., 2006. Microbial carbonate abundance compared with fluctuations in metazoan diversity over geological time. Sedimentary Geology 185, 229–238.

Riding, R., Liang, L., 2005. Geobiology of microbial carbonates: metazoan and seawater saturation state influences on secular trends during the Phanerozoic. Palaeogeography, Palaeoclimatology, Palaeoecology 219, 101–115.

Rowland, S., Shapiro, R.S., 2002. Reef patterns and environmental influences in the Cambrian and earliest Ordovician. In: Kiessling, W., Flügel, E. (Eds.), Phanerozoic reef patterns: SEPM Special Publication, 72, pp. 95–128.

Sandberg, P.A., 1983. An oscillating trend in non-skeletal carbonate mineralogy. Nature 305, 19–22.

Scotese, C.R., McKerrow, W.S., 1991. Ordovician plate tectonic reconstructions. Advances in Ordovician geology: In: Barnes, C.R., Williams, S.H. (Eds.), Geological Survey of Canada Paper, vol. 90–9, pp. 271–282.

Sepkoski, J.J., 1996. Patterns of Phanerozoic extinction: a perspective from global data bases. In: Walliser, O.H. (Ed.), Global Events and Event Stratigraphy. Springer-Verlag, Berlin, pp. 35–52.

Shapiro, R.S., 1995. Mollusc-stromatolite/thrombolite synecology in the Late Cambrian–Early Ordovician of the Great Basin — a preliminary report (abstract): California Paleontology Conference, Abstracts and Fieldtrip Guidebook, Bishop, California, 10–11.

Shapiro, R.S., 2000. A comment on the systematic confusion of thrombolites. Palaios 15, 166–169.

Shapiro, R.S., Awramik, S.M., 2006. *Favosamaceria Cooperi* new group and form: a widely dispersed, time-restricted thrombolite. Journal of Paleontology 80, 411–422.

Strasser, A., 1986. Ooids in Purbeck limestones (lowermost Cretaceous) of the Swiss and French Jura. Sedimentology 33, 711–727.

Walker, R.G., Plint, A., 1992. Wave- and storm-dominated shallow marine systems. In: Walker, R.G., James, N.P. (Eds.), Facies models: response to sea level change. Geological Association of Canada, Newfoundland, pp. 219–238.

Wilson, M.A., Palmer, T.J., 1992. Hardground and hardground faunas. University of Wales, Aberystwyth, Institute of Earth Studies Publication 9 (131 pp.).

Woo, J., Chough, S.K., 2007. Depositional processes and sequence stratigraphy of the Jigunsan Formation (Middle Ordovician), Taebaeksan Basin, mideast Korea: implications for basin geometry and sequence development. Geosciences Journal 11, 331–355.

Woo, J., Chough, S.K., 2010. Growth patterns of the Cambrian microbialite: phototropism and speciation of *Epiphyton*. Sedimentary Geology 229, 1–8.

Zhuravlev, A.Y., 1996. Reef ecosystem recovery after the Early Cambrian extinction, In: Hart, M.B. (Ed.), Biotic recovery from mass extinction events. Geological Society of London Special. Publication 102, 79–96.

Zhuravlev, A.Y., Wood, R.A., 1996. Anoxia as the cause of the mid-Early Cambrian (Botomian) extinction event. Geology 24, 311–314.

Zhuravlev, A.Y., Wood, R.A., 2008. Eve of biomineralization: controls on skeletal mineralogy. Geology 36, 923–926.